ELSEVIER

Journal of Electroanalytical Chemistry 449 (1998) 67–80

JOURNAL OF ELECTROANALYTICAL CHEMISTRY

A chemical and electrochemical study of titanium ions in the molten equimolar $CaCl_2 + NaCl$ mixture at 550°C.

A.M. Martínez [a], Y. Castrillejo [a,*], E. Barrado [a], G.M. Haarberg [b], G. Picard [c]

[a] Dpto. de Química Analítica, Facultad de Ciencias, Universidad de Valladolid, Prado de la Magdalena s/n, 47005 Valladolid, Spain
[b] Department of Electrochemistry, Norwegian University of Science and Technology, Trondheim-7034, Norway
[c] Laboratoire d'Electrochimie Analytique et Appliquée, Ecole Nationale Superieure de Chimie de Paris, 11 rue Pierre et Marie Curie, 75231 Cedex 05, France

Received 27 May 1997

Abstract

The chemical and electrochemical properties of solutions of titanium chlorides in the fused $CaCl_2 + NaCl$ equimolar mixture were studied at 550°C using different working electrodes. We determined the stability range of the various oxidation states of titanium and calculated the standard potentials of the Ti(III)/Ti(II) and Ti(II)/Ti(0) redox couples, the solubility products of the titanium oxides, the kinetic parameters of the electrochemical systems at the different electrodes and the diffusion coefficients of the electroactive species. We have also studied the titanium electrodeposition process by potential step measurements which indicated instantaneous nucleation of titanium at tungsten substrates. All these data allowed us to build-up the potential-pO^{2-} diagram which summarizes the properties of Ti-O compounds in the melt studied and can be used (together with the E-pO^{2-} diagram of chlorinating gaseous mixtures) to predict operating conditions for the process of industrial production of metallic titanium from molten salt systems.

Keywords: Molten chlorides; Refractory metals; Titanium chlorides; Titanium electrodeposition; Kinetic parameters; Solubility products; E-pO^{2-} diagrams

1. Introduction

Besides the well known industrial production of metallic titanium based on metallothermic reduction of $TiCl_4$ (Kroll process [1]), an alternative process that employs molten $TiCl_4$ + alkali chloride baths at low temperatures has been sought since the early 1950s. Thus the electrodeposition of titanium from molten salt systems has been investigated by many researchers [2–7] using either alkali chloride or alkali fluoride + chloride based systems at temperatures from 450 to 850°C using $TiCl_4$ as the raw material.

However, important discrepancies between the various results available in the literature have been found. This is because the electrodeposition process of titanium is very complicated due to the lower valent compounds of titanium (Ti^{2+}, Ti^{3+}) which exist in the electrolytic bath and the reactions between metallic titanium and tetra- or trivalent titanium ions [8–11]. It has been demonstrated by several workers [12,13] that an equilibrium exists between the three constituents (Ti, $TiCl_2$ and $TiCl_3$) and that the equilibrium:

$$Ti + 2Ti(III) \Leftrightarrow 3Ti(II) \quad (1)$$

is displaced far to the right in most alkali chloride melts.

On the other hand, the different oxidation states of titanium are interrelated by four disproportionation reactions which may occur simultaneously according to Chassaing et al. [14]:

$$3TiCl_2 \Leftrightarrow Ti + 2TiCl_3 \quad (2)$$

* Corresponding author. Tel.: +34 983 423000.

0022-0728/98/$19.00
PII S0022-0728(97)00413-0

$$2TiCl_3 \Leftrightarrow TiCl_2 + TiCl_4 \quad (3)$$

$$4TiCl_3 \Leftrightarrow Ti + 3TiCl_4 \quad (4)$$

$$2TiCl_2 \Leftrightarrow Ti + TiCl_4 \quad (5)$$

The above reactions are heterogeneous (solid Ti metal, gaseous $TiCl_4$ in equilibrium with the soluble complex M_2TiCl_6). The workers obtained marked dependence on the experimental conditions such as temperature, nature of the atmosphere, surface area of the titanium exposed and the nature of the cation in the molten alkali chloride at 700°C.

In fluoride + chloride mixtures, Ti(III) is supposed to be reduced directly to the metal [15] and in pure fluoride melts (FLINAK), the TiF_6^{2-} species was found to be reduced to titanium metal from Ti(III) [16]. These studies indicated that there were differences in behaviour of Ti ions in the two solvent systems, i.e. chlorides and fluorides. Notably, there was the non-existence of an intermediate reduction step involving Ti(II) in fluoride or chloride + fluoride molten salts.

The kinetics of the electrodeposition and electrocrystallization of titanium were studied in alkali chloride melts [17,18]. The studies were performed in dilute solutions of $TiCl_2/TiCl_3$ in binary mixtures of LiCl + KCl eutectic and NaCl + KCl eutectic, in NaCl and also in KCl + LiCl + NaCl (40:20:40 mol%). Well defined voltammetric peaks corresponding to the reduction step $Ti(II) + 2e^- \Leftrightarrow Ti$ and the subsequent anodic dissolution of the deposit but ill-defined peaks for the red-ox $Ti(III) + e^- \Leftrightarrow Ti(II)$ exchange were obtained. The cathodic reduction Ti(III)/Ti(II) was found to be irreversible while the Ti(II)/Ti reduction was quasi-reversible.

Chemical and electrochemical properties of titanium compounds in molten LiCl + KCl eutectic at 470°C have been studied extensively by Ferry et al. [19,20]. They demonstrated that operating conditions for selective chlorination in molten salts of a complex ore can be predicted from fundamental data for the oxoacidic, oxobasic and redox properties of the components of the ore and of gaseous reagents in the melt, indicating that a low-temperature molten-salt process for the treatment of ilmenite or rutile and the subsequent electrowinning of titanium from the resulting melt solution of titanium (IV) chloride should be feasible.

In addition to studies in chloride (both binary and ternary systems) and fluoride systems, Vire [21] also investigated electrolysis of titanium from Ti_2O_3 + NaF and Ti_2O_3 + cryolite mixtures. Electrochemical studies of titanium have also been performed in molten sodiumtetrafluoroborate ($NaBF_4$) at 420°C by Claiton and Mamantov [22] and by Schlain [23] in $NaBO_2$ and $LiBO_2$ melts containing small amounts of titanium oxides. Okada et al. [24] made studies of titanium chlorides in $LiNO_3$ (mp 132°C) and $NaNO_3$ (mp 218°C).

Moreover, electrochemical studies in molten $AlCl_3$ + alkali halides have received considerable attention in the last two decades [25]. Due to their acid-base character combined with the low liquidus temperatures, chloroaluminate are good media for studying unusually low oxidation states.

The purpose of our investigation was to determine fundamental data necessary to conceive a process including both treatment of titanium ores and subsequent electrowinning of metallic titanium in a single melt. Results from electrochemical experiments associated with thermodynamic data of the literature allowed us to set up potential-oxoacidity (pO^{2-}) diagrams summarizing the properties of Ti-O compounds and of chlorinating gaseous mixtures in molten $CaCl_2$ + NaCl equimolar mixture at 550°C. Analysis of these diagrams led to a forecast of operating conditions for performing the aimed process. Moreover we have undertaken a systematic study of the electrochemistry of titanium. In this way, we have studied both the Ti(III)/Ti(II) and Ti(II)/Ti(0) systems in order to have at our disposal fundamental data for the last stage of the molten salt process for titanium extractive metallurgy.

2. Experimental

2.1. Apparatus and purification of the melt

The equimolar mixture ($CaCl_2$ and NaCl analytical grade) was melted in a 100-cm^3 alumina crucible placed in a quartz cell inside a furnace. The temperature of the furnace was controlled to ±2°C by a West 3300 programmable device. All handling of the salts was done inside a glove box.

The mixture was fused under vacuum, then raised to atmospheric pressure using dry argon, purified by bubbling HCl through the melt for at least 30 min, and then kept under argon atmosphere [26].

2.2. Electrodes

The pO^{2-} indicator electrode consisted of a tube of yttria-stabilized zirconia, supplied by Degussa (inner diam. 4 mm; outer diam. 6 mm), filled with molten $CaCl_2$ + NaCl and containing oxide and silver ions in which a silver wire was immersed (inner reference $Ag|Ag^+$). The reference electrode consisted of a silver wire (0.5 mm diameter) dipped into a quartz tube containing a solution of silver chloride in $CaCl_2$ + NaCl.

The 1-mm diameter tungsten and molybdenum wires and 3 mm glassy carbon rods were used as working electrodes.The counter electrode was a tungsten wire or a graphite rod. The electrode active surface area was determined by the depth of immersion and corrected for the height of the meniscus.

2.3. Preparation of titanium solutions

The chemical stability of solutions is an important parameter which must be controlled to ensure reproducible electrochemical measurements.

The experimental problems related to the low solubility of $TiCl_4$ prevented the preparation of stable solutions of Ti(IV), which is quickly lost from the melt. The 'in situ' reduction of this compound by hydrogen to obtain $TiCl_3$ requires a complex experimental device and it is hard to know the exact amount of salt introduced to the melt, for which the Ti(III) solutions were always prepared by direct addition of weighed amounts of solid $TiCl_3$ which was kept in a dry glove box until its use, stored under an argon atmosphere and used without further purification.

Ti(II) solutions were prepared by two different ways: (i) anodic dissolution of a high-purity titanium wire (Aldrich, 99.99%, 1-mm diameter) at constant current, which is the technique currently used in our laboratory. During coulometric experiments a tungsten spiral foil was used as a counter electrode which was separated from the melt by a quartz tube with a glass frit. To ensure that Ti(II) is the anodization product, the weight loss of the titanium wire was determined after the passage of a certain charge. (ii) Addition of $TiCl_3$ in the presence of excess of metallic titanium to allow the following equilibrium:

$$2TiCl_3 + Ti \Leftrightarrow 3TiCl_2 \quad (6)$$

to be established. This has already been used in other molten chlorides [17–20]. The progress of the reaction was followed by voltammetry. The voltammetric properties of these solutions were identical to those of solutions prepared by anodizing titanium metal as described above.

2.4. Determination of titanium

The total concentration of dissolved titanium was confirmed by taking samples during and at the end of the experiments and then analyzed by gravimetric analysis as following. The sample containing Ti(III) or Ti(II) ions was dissolved in water with 1:1 (v/v) hydrochloric acid and addition of concentrated HNO_3 to make sure that all the titanium exists as Ti(III). NH_3 is added until the solution is nearly neutral (a point were the solution is lightly turbid, the precipitate dissolving upon vigorous stirring). First, 5 cm^3 of glacial acetic acid followed by 15 g of ammonium acetate or its equivalent in solution was added and the volume of the solution was made up to about 350 cm^3. The solution was brought rapidly to boiling and maintained in ebullition for about 3 min. The titanium will precipitate in a white, flocculent and readily filterable condition. The precipitate is washed first with water containing acetic acid and finally with pure water. The filter and the precipitate were firstly dried cautiously at approximately 120°C and then ignited over an oven (temperature $\approx$800°C). The residue is weighed as TiO_2.

2.5. pK_i determinations

With the reference and zirconia electrodes placed in the melt, a known amount of Ti(III) or Ti(II) was titrated with oxide ions added as sodium carbonate which dissociates completely into O^{2-} and gaseous carbon dioxide [26]. Continuous stirring with dried argon was required and the carbonate additions were made every hour (that corresponds to the stabilization of the potential after each addition)

2.6. Electrochemical apparatus

Cyclic voltammograms were obtained with a PAR EG&G Model 273A potentiostat/galvanostat controlled by the PAR EG&G M270 4.10 software package. The simulated voltammograms were recorded with M271 COOL kinetic analysis software (PAR).

The emf measurements were performed with a high impedance voltmeter Crison 2002 and the coulometric experiments were conducted by the use of a Metrohm Herisau Coulostat E524 apparatus.

3. Results and discussion

3.1. Electrochemistry of titanium

3.1.1. Characterization of the voltammetric waves: stable oxidation states

Special attention was devoted to the working electrode material. The anodic and cathodic limiting processes in the melt are chlorine evolution and alkali metal deposition respectively [27]. The theoretical useful potential range of the melt is 3.585 V, which can be calculated from the thermodynamic data. In fact, ΔE is related to the Gibbs energy change ΔG in the reaction:

$$Na + 1/2Cl_2 \leftrightarrow NaCl \quad (7)$$

by the classical relation:

$$\Delta G = -nF\Delta E \quad (8)$$

The value of ΔG is easily determined from the Gibbs energy ΔG^0 of the reaction involving pure compounds, and from the activity of NaCl in melt: $a_{NaCl} = 0.27$ at 550°C [28].

We tried to find an electrode material which had such a wide range of electrochemical stability. The working electrode materials were tungsten, molybdenum and glassy carbon. Tungsten does not alloy with the alkali metals.The experimental electroactivity range obtained

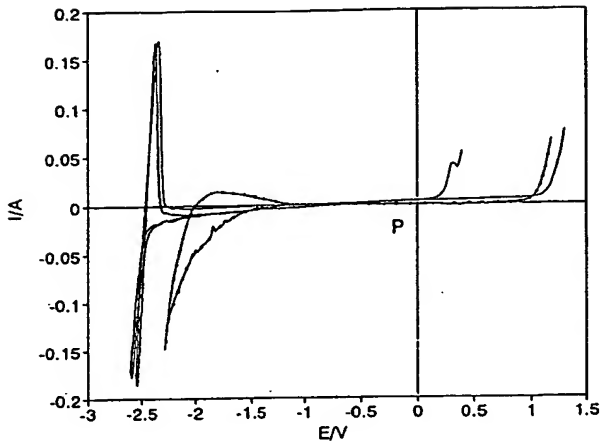

Fig. 1. Cyclic voltammograms obtained at tungsten (0.25 cm^2), molybdenum (0.28 cm^2), and glassy carbon (· · ·) (0.82 cm^2), electrodes in pure $CaCl_2$ + NaCl melt. Sweep rate 0.2 V s^{-1}.

by extrapolating the limiting anodic polarization curve to zero current (see Table 1) is higher than the theoretical value, indicating an electrochemical reaction overvoltage for chlorine evolution. Molybdenum exhibits a high degree of electrochemical stability, but its practical oxidation potential is different from the value of chlorine evolution, indicating that molybdenum can be dissolved anodically; similar behaviour was observed by some authors in other molten chlorides [29]. In addition, glassy carbon is useful for studying reactions involving the highest oxidation states of the electroactive species and the oxidation of the chlorine ions which constitute the anodic limit of the solvent. At negative potentials the limiting processes are underpotential deposition of sodium and calcium carbide (see Table 1, Fig. 1).

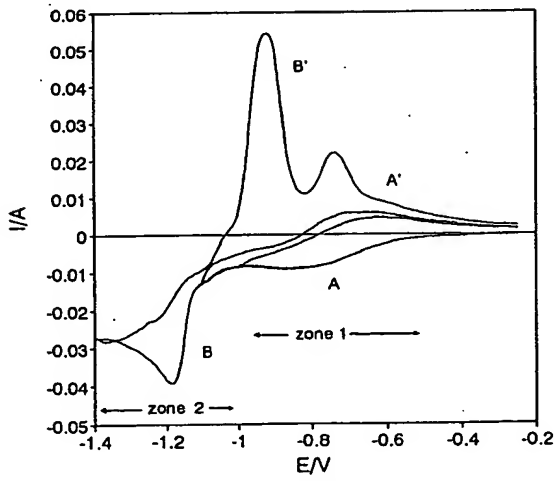

Fig. 2. Typical cyclic voltammogram for the reduction of titanium trichloride ($2.21 \cdot 10^{-4}$ mol cm^{-3}) on a tungsten electrode at different shift potentials. Sweep rate 0.2 V s^{-1}. S = 0.22 cm^2.

Table 1
Electrochemical window of the equimolar $CaCl_2$ + NaCl at the different substrates

	Glassy carbon	Molybdenum	Tungsten
$\Delta E/V$ versus Cl_2/Cl^-	3.400 ± 0.030	2.800 ± 0.030	3.620 ± 0.030

Typical voltammograms for the reduction of Ti(III) solutions are shown in Fig. 2. The voltammograms show the same general features at tungsten, molybdenum and glassy carbon where the reduction of titanium trichloride takes place in two steps. In zone 1, the cathodic wave A associated with the anodic wave A', which shapes are characteristic of a soluble-soluble exchange, are related to the Ti(III)/Ti(II) exchange. Moreover, zone 2 shows a cathodic peak B and one sharp anodic stripping peak B' characteristic of a system involving an insoluble compound; it corresponds to the Ti(II)/Ti(0) system. This was confirmed in different ways: (i) working with a pure titanium metal electrode in a solution containing Ti(II) ions the voltammograms showed that the potential domain for titanium formation falls in the same range as those observed in Fig. 2.; and (ii) the deposit of the metal obtained under potentiostatic conditions consisted of pure metallic titanium which was determined by energy dispersive X-ray analysis using the scanning electron microscope (Fig. 3).

We have also used square wave voltammetry (SWV) to investigate the stable oxidation states of titanium in the $CaCl_2$ + NaCl melt. This technique was described in detail by Osteryoung et al. [30] and Ramaley et al. [31]. The potential-time function consists of the sum of a synchronized square wave and of a staircase potential ramp. The current is sampled at the end of every half wave and then differentiated. This allows capacitive and residual currents to be eliminated and makes the method highly sensitive.

For a simple reversible reaction, the net current-potential curve is bell-shaped and symmetrical about the half-wave potential, and the peak height is proportional to the concentration of the electroactive species. Whenever there is any interference between the peaks, deconvolution software can be used to separate the total signal into its components.

According to Baker et al. [32] and Osteryoung et al. [33] the width of the half-peak, $W_{1/2}$, depends on the number of electrons exchanged and on the temperature as follows:

$$W_{1/2} = 3.52RT/nF \quad (9)$$

This equation corresponds to a reversible exchange, but we can choose the appropriate experimental conditions (i.e. frequency of the square signal) where the system behaves reversibly.

Fig. 3. SEM micrograph showing titanium deposited under potentiostatic conditions (−1400 mV).

Fig. 4 presents a net-current square wave voltammogram for the reduction of a Ti(III) solution at a tungsten electrode. The n-values obtained are close to 1 and 2, which confirms that the exchanges are Ti(III)/Ti(II) and Ti(II)/Ti(0), respectively.

No existence of Ti(IV)/Ti(III) exchange was observed, probably due to the low solubility of gaseous $TiCl_4$.

On the contrary, when the experiments were carried out in the eutectic LiCl + KCl we could see an anodic peak associated with a narrow cathodic peak corresponding to the oxidation of Ti(III) to Ti(IV) which leads to the formation of the insoluble Li_2TiO_3 giving the sharp peak during the reverse scan which is characteristic

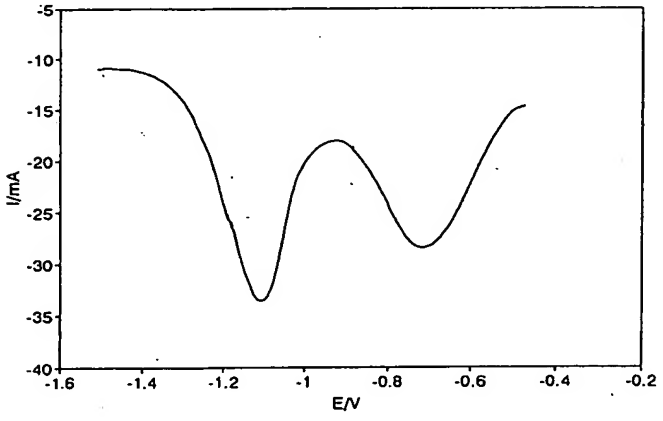

Fig. 4. Net-current square wave voltammograms for the reduction of Ti(III) at a tungsten electrode in $CaCl_2$ + NaCl (T = 550°C). Pulse height: 25 mV; potential step: 1 mV; frequency: 60 Hz. S = 0.22 cm^2.

of the formation of a solid compound adhered to the electrode. A similar behaviour was observed by Ferry el al. [19,20]. However, they claim that the existence of the sharp peak was assumed to the formation of gaseous Ti(IV) by oxidation of Ti(III).

The A/A′ and B/B′ exchanges were studied separately.

3.1.2. Ti(III)/Ti(II) exchange

A detailed investigation of the Ti(III)/Ti(II) redox system (Peaks A/A′) was performed. A series of normalized voltammograms was recorded in an equimolar $CaCl_2$ + NaCl purified bath containing $TiCl_3$, for a variety of concentrations and sweep rates, by using different substrates. As an example, Fig. 5a shows the cyclic voltammograms obtained at a tungsten electrode. In all cases, plots of the negative peak current versus the square root of the sweep rate were found to be linear which indicates that the reaction is diffusion controlled (Fig. 5b). From the slope of such plots, the diffusion coefficient of Ti(III) ions has been calculated and the values obtained are collected in Table 2.

Analysis of the voltammograms showed that the potential peak does not change with increasing sweep rate for values up to 0.5 $V\,s^{-1}$ (Fig. 5c), whereas at higher scan rates it shifted to more negative potentials. This is probably due to the non-reversibility of the process. Estimation of the value of the transfer coefficient, α, was then possible (Table 3) by applying the equation:

$$\Delta E_p/\Delta \log v = 2.3RT/2\alpha nF \quad (10)$$

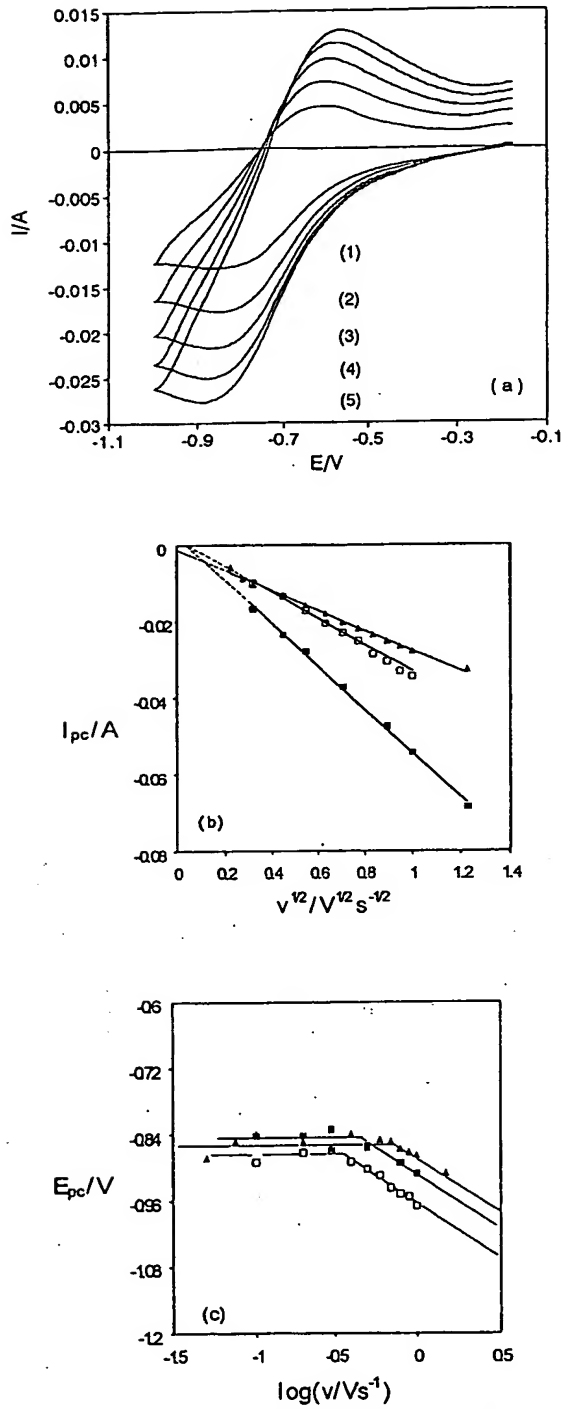

Fig. 5. (a) Cyclic voltammograms for the Ti(III) reduction at a tungsten electrode. Sweep rates: v/V s^{-1} (1) 0.2; (2) 0.3; (3) 0.4; (4) 0.5; (5) 0.6. (b) Variation of the cathodic current peak with the square root of the sweep rate corresponding to the voltammograms for Ti(III)/Ti(II). (c) Variation of the cathodic peak potentials with the logarithm of the sweep rate corresponding to the voltammograms for Ti(III)/Ti(II). Experimental conditions: (▲) Tungsten: S = 0.22 cm^2; $[TiCl_3] = 2.21 \cdot 10^{-4}$ mol cm^{-3}. (■) Molybdenum: S = 0.25 cm^2; $[TiCl_3] = 4.44 \cdot 10^{-4}$ mol cm^{-3}. (□) Glassy carbon: S = 0.67 cm^2; $[TiCl_3] = 8.00 \cdot 10^{-4}$ mol cm^{-3}.

Table 2
Titanium(III) diffusion coefficients obtained on each substrate by different electrochemical techniques

TECHNIQUE	$10^5 D/cm^2 s^{-1}$		
	Glassy carbon	Molybdenum	Tungsten
Voltammetry	(1.0 ± 0.1)	(1.0 ± 0.1)	(0.99 ± 0.01)
Convolution	(1.3 ± 0.1)	(1.2 ± 0.1)	(1.6 ± 0.1)

Table 3
Values of the charge-transfer coefficient, α, for the Ti(III)/Ti(II) exchange obtained by means of Eq. (10), at different substrates

Working electrode	α
Tungsten	0.49 ± 0.05
Molybdenum	0.53 ± 0.05
Glassy carbon	0.37 ± 0.05

In addition, the linear potential sweep data were transformed, according to the convolution principle [34,35], into a form resembling a steady-state voltammetric curve. The main advantage that can be expected from the use of convolution procedures in treating the voltammogram data is that the accuracy in the mechanism determination is better, since the information available along the whole I–E curve is used instead of only the peak values. The semi-integrals for some voltammetric curves are shown in Fig. 6. When viewing the convoluted curves, one observes the occurrence of a plateau proving diffusion control. Moreover, the convoluted curves were very similar when increasing the sweep rate, but the direct and reverse scans were not identical for any of the substrates studied, which is probably due to some irreversibility of the Ti(III)/Ti(II)

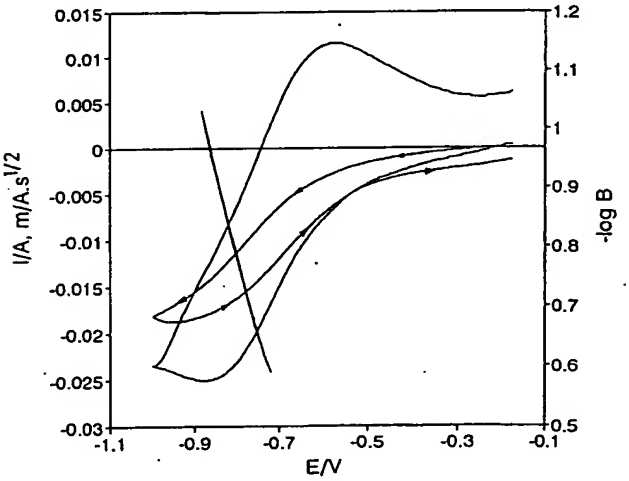

Fig. 6. Cyclic voltammogram, its corresponding convoluted curve and the logarithmic analysis of the convoluted data following a quasi-reversible model. Sweep rate: 0.8 V s^{-1}.

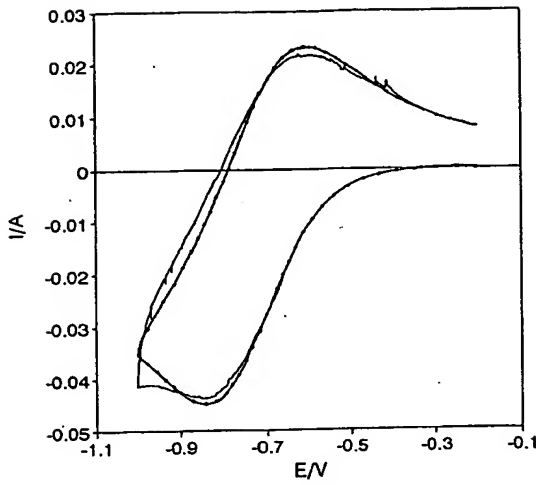

Fig. 7. Cyclic sweep voltammogram of $TiCl_3$ reduction at a glassy carbon electrode. (——) Experimental results; (· · ·) simulated results corresponding to a quasi-reversible process. Sweep rate, 0.9 V s^{-1}.

process. On the other hand, the diffusion coefficient of Ti(III) was obtained when the transformed current data reached the limiting values from the equation:

$$m^* = nFSc_oD^{1/2} \quad (11)$$

where m^* is the maximum of the semi-integral of the voltammetry current, c_o is the bulk concentration of the electroactive species, D is the diffusion coefficient and S is the electrode surface area (see Table 2).

In addition, we have carried out the rigorous analysis of the convoluted curves according to quasi-reversible reaction, by applying the equation [36]:

Table 4
Kinetic parameters of Ti(III)/Ti(II) exchange obtained from the analysis of the convoluted curves according to a quasi-reversible model

Substrate	Log ($k°$/cm s^{-1})	α
Tungsten	-1.88 ± 0.04	0.48 ± 0.04
Molybdenum	-1.88 ± 0.20	0.39 ± 0.08
Glassy carbon	-1.89 ± 0.08	0.40 ± 0.02

Table 5
Values of the kinetic parameters corresponding to the Ti(III)/Ti(II) exchange calculated by using the M271 COOL simulation computer program, at different electrodes

Substrate	$E_{1/2}$/V	Log ($k°$/cm s^{-1})	α
Tungsten	$-(0.718 \pm 0.001)$	-2.18 ± 0.04	0.40 ± 0.03
Molybdenum	$-(0.727 \pm 0.009)$	-1.91 ± 0.31	0.37 ± 0.09
Glassy carbon	$-(0.717 \pm 0.006)$	-2.28 ± 0.04	0.41 ± 0.02

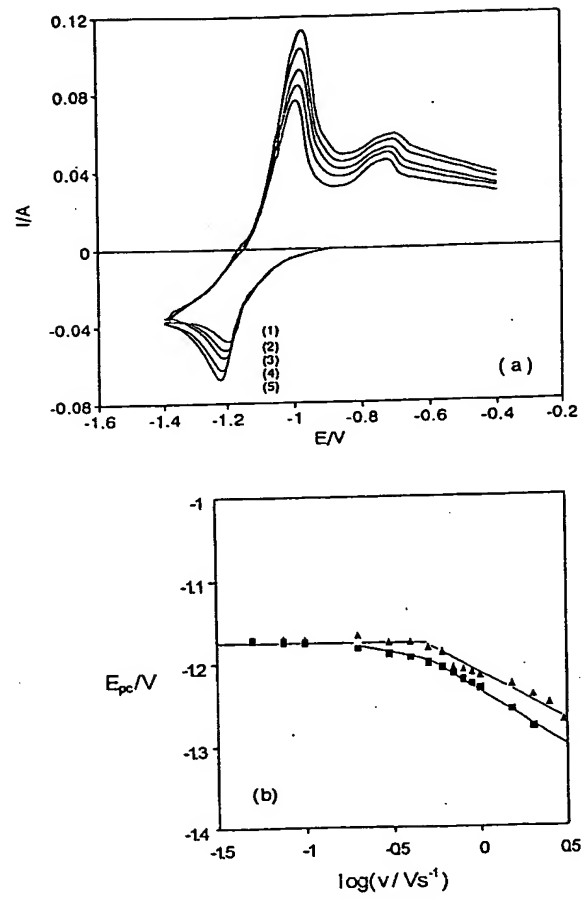

Fig. 8. (a) Cyclic voltammograms obtained on a molybdenum electrode showing the reduction of Ti(II). Sweep rates: v/V s^{-1} (1) 0.2; (2) 0.3; (3) 0.4; (4) 0.5; (5) 0.6. $TiCl_2$ concentration: $1.6 \cdot 10^{-4}$ mol cm^{-3}. Electrode area: 0.38 cm^2. (b) Variation of the cathodic peak potential with the logarithm of the sweep rate. (▲) Tungsten, and (■) molybdenum electrodes.

$$E = E_2^\circ + (2.3RT/\alpha nF)\log(k°/D^{1/2}) + (2.3RT/\alpha nF)\log B \quad (12)$$

where

$$B = [m^* - m - m\exp\{(nF/RT)(E - E_2^\circ)\}]/I \quad (13)$$

$k°$ and α are the charge transfer rate constant and the transfer coefficient respectively, m is the convoluted current and E_2° is the standard potential of the Ti(III)/Ti(II) system which was estimated from voltammetric measurements by applying the relationship: $(E_{pa} + E_{pc})/2$ (assuming that the Ti(III) and Ti(II) diffusion coefficients are similar, which will be confirmed later on).

The average values of $k°$ and α obtained from the plot of E versus the logarithmic function of convoluted current are gathered in Table 4. According to the criteria of Matsuda and Ayabe [37], the exchange Ti(III)/Ti(II) can be classified as quasi-reversible at all the substrates studied.

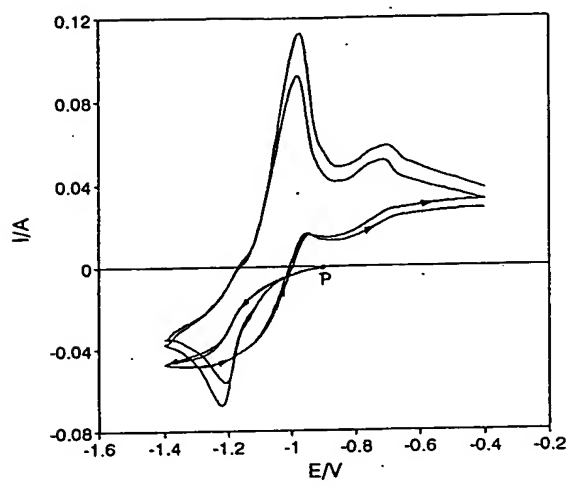

Fig. 9. Several cyclic voltammograms and their corresponding convoluted curves obtained at a molybdenum electrode. Sweep rates: (1) 0.4 and (2) 0.6 V s^{-1}.

In order to confirm these results, we have used a simulation computer program (M271 COOL kinetic analysis software 1.10 from PAR) [38], for a quasi-reversible mechanism in which the charge-transfer rate constant, k°, the transfer coefficient, α, and the half-wave potential, $E_{1/2}$, were adjusted to give the best fit between the experimental and calculated results. We also tried to fit the system to a reversible process. However the best results were found for a quasi-reversible process. Representative examples of these simulations are shown in Fig. 7 and the average values obtained are in Table 5. Comparing the values from Tables 4 and 5, it is possible to see the very good agreement between the different methods employed.

3.1.3. Study of titanium electrodeposition

The Ti(II)/Ti(0) exchange has been studied at the metallic electrodes W and Mo.

The cathodic peak has the characteristics of a diffusion controlled process (steep rise and slow decay). The anodic peak also has the expected characteristics, in this case those of a stripping peak (decay steeper than rise). The ratios of the forward-to-reverse current peaks (I_{pa}/I_{pc}) are higher that unity, and the ratio Q_a/Q_c remains approximately constant at unity with increasing sweep rates, which indicates that all the deposited material is removed electrochemically during the positive sweep, that the Ti adhesion to the electrode surface was good, and also that there are no conflicting chemical reactions coupled to the primary electrochemical process.

Table 6
Values of the kinetic parameters corresponding to the Ti(II)/Ti(0) exchange calculated by means of the logarithmic analysis of the convoluted curves

Substrate	Log (k°/cm s^{-1})	α
Tungsten	-3.96 ± 0.35	0.59 ± 0.08
Molybdenum	-3.77 ± 0.64	0.59 ± 0.14

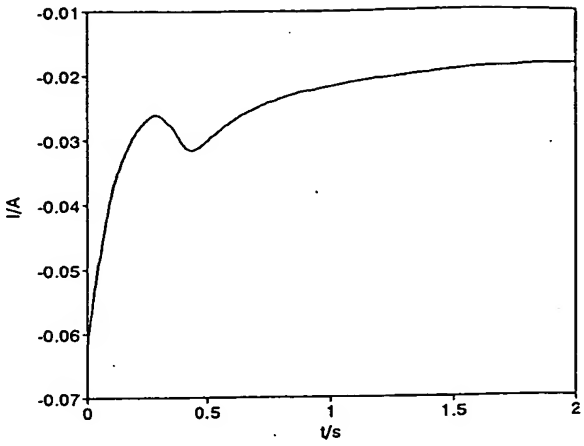

Fig. 10. Example of current transient for electrochemical deposition of titanium on a tungsten electrode. Potential step: −1.20 V.

Overall, the voltammetric peaks for the deposition and stripping of titanium at tungsten and molybdenum electrodes are unremarkable in appearance. However, in both cases the voltammetric curves recorded at different sweep rates (Fig. 8a), clearly show that the cathodic peak potential, E_{pc}, (Fig. 8b) shifts negatively, and the peak potential half-peak potential separation [$E_{pc} - E_{p/2}$], increases when the sweep rate is increased ($v > 0.5$ and 0.7 V s^{-1} at molybdenum and tungsten electrodes respectively) giving values higher than expected for reversible and purely diffusion controlled processes, suggesting some irreversibility of the Ti(II)/Ti(0) system.

In order to confirm these results we have performed the semi-integration of the voltammograms. The convoluted curves obtained were very similar for the whole sweep rate range studied, however they do not remain identical from the direct to reverse scan as it can be observed in Fig. 9, showing the non-reversibility of the titanium deposition.

Table 7
Ti(II) diffusion coefficients obtained by different electrochemical techniques at different solid substrates

Technique	$10^5 D$/cm^2 s^{-1}	
	Tungsten	Molybdenum
Voltammetry	(0.67 ± 0.03)	(0.62 ± 0.03)
Convolution	(1.7 ± 0.2)	(1.6 ± 0.2)
Chronopotentiometry	(1.8 ± 0.2)	—

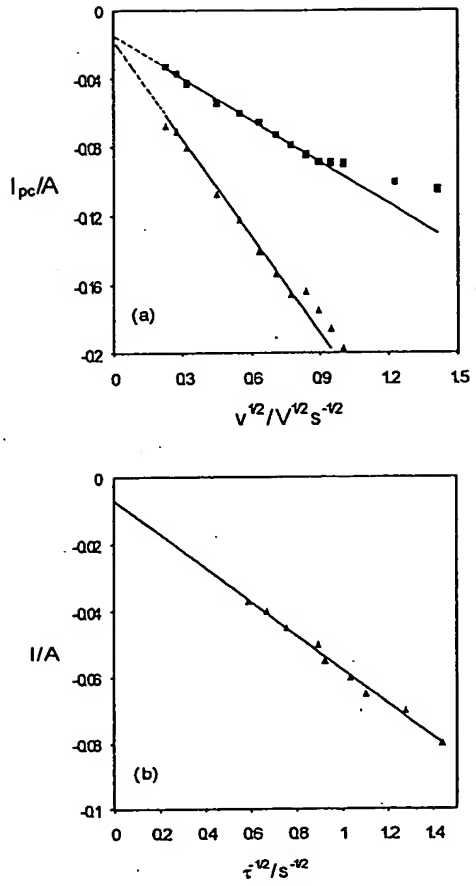

Fig. 11. (a) Variation of the cathodic current peak with the square root of the sweep rate corresponding to voltammograms from Fig. 9. Experimental conditions: (▲) Tungsten: $S = 0.35$ cm^2; $[TiCl_2] = 3.3 \cdot 10^{-4}$ mol cm^{-3}. (■) Molybdenum: $S = 0.38$ cm^2; $[TiCl_2] = 1.6 \cdot 10^{-4}$ mol cm^{-3}. (b) Verification of the Sand's law.

When the convoluted curves were analyzed further, we could extract an interpretation of the mechanism and the estimation of kinetic parameters by plotting the logarithmic function of convoluted current corresponding to a quasi-reversible exchange with formation of an insoluble product as a function of E [39]:

$$E = E_1^\circ + (2.3RT/\alpha nF) \log k^\circ + (2.3RT/\alpha nF) \log A \quad (14)$$

A being,

$$A = [(m^* - m)D^{-1/2} + nFS \exp\{(nF/RT)(E - E_1^\circ)\}]/I \quad (15)$$

where E_1° is the standard potential of the Ti(II)/Ti(0) system and was calculated by voltammetry applying the following equation [34]:

$$E_p = E_1^\circ + (2.3RT/nF) \log c_o - 0.849(RT/nF) \quad (16)$$

to those conditions where the electrochemical reaction is diffusion controlled, E_p being the cathodic peak potential, c_o the bulk concentration and n the number of electrons exchanged. R and T have the usual meanings.

The values of the kinetic parameters so obtained confirmed the quasi-reversibility of the Ti(II)/Ti(0) exchange at molybdenum and tungsten substrates (see Table 6).

A further study of the electrochemical behaviour of Ti(II) was carried out by using chronopotentiometry. Logarithmic analysis of chronopotentiograms was carried out: plots of the electrode potentials versus $\log[1 - (t/\tau)^{1/2}]$ were linear, but the slopes of the linear part of the curves were different from the theoretical value for a two-electron reversible exchange process (0.0816 V (decade)$^{-1}$) at 550°C.

Moreover, I–t transients suggest that nucleation of metallic titanium on a tungsten electrode dominates the electrodeposition process. The appearance of these curves indicated that nucleation and growth phenomena play a part in the overall deposition process (Fig. 10): each transient exhibits a charging current spike concurrent with the onset of the potential step followed

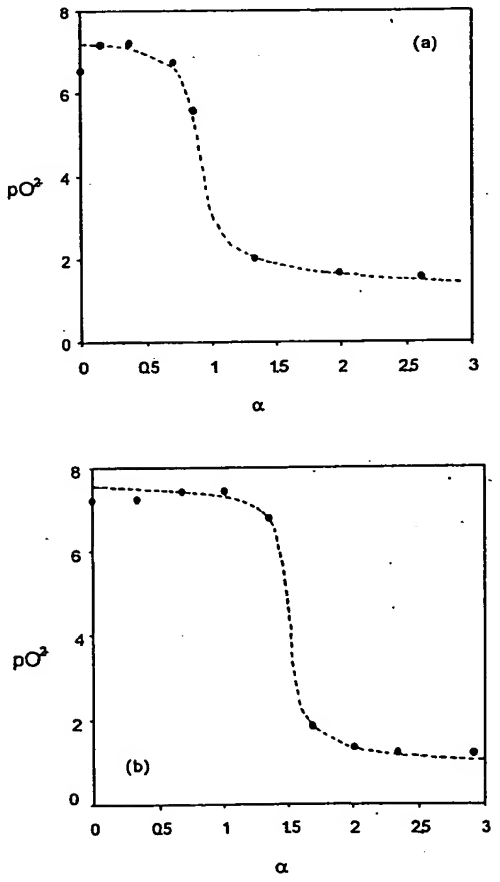

Fig. 12. (a) Potentiometric titration curve of 0.0108 mol kg^{-1} Ti^{+2} solution by O^{2-} ions added as solid Na_2CO_3. (b) Potentiometric titration of Ti^{+3} solution (0.0248 mol kg^{-1}) by O^{2-} ions.

Table 8
Solubility products of titanium oxides in the equimolar $CaCl_2$+NaCl mixture at 550°C

Equilibrium	Expression for solubility product	Stability constant, pK_s (molal scale)
$TiO(s) \leftrightarrow Ti^{+2}+O^{2-}$	$K_{s,1}=[Ti^{+2}][O^{-2}]$	9.01 (a) 9.82 (b)
$Ti_2O_3(s) \leftrightarrow 2Ti^{+3}+3O^{2-}$	$K_{s,2}=[Ti^{+3}]^2[O^{-2}]^3$	25.7 (a) 25.8 (b)
$TiO_2(s) \leftrightarrow Ti^{+4}+2O^{2-}$	$K_{s,3}=[Ti^{+4}][O^{-2}]^2$	19.62 (b, rutile) 8.91 (b, anatase)

(a) Values obtained from potentiometric titration.
(b) Values calculated from thermodynamic data.

by a rising current due to the nucleation and growth of titanium nuclei. The rising current reaches a maximum, I_M, as the individual diffusion zones of the growing nuclei merge. The position of this maximum on the time axis, t_M, depends on the magnitude of the potential step, and decreases as the applied potential is more negative.

The most interesting part of the cathodic $I-t$ transients is the rising portion of the curves which obeyed an I against $t^{1/2}$ linear relationship demonstrating that initial stages of electrochemical deposition of titanium at a tungsten electrode can be explained in terms of a model involving instantaneous nucleation [40].

This result is in agreement with Haarberg et al. [18] who studied the electrodeposition of titanium from chloride melts and found instantaneous nucleation and growth of titanium nuclei at tungsten and stainless steel substrates.

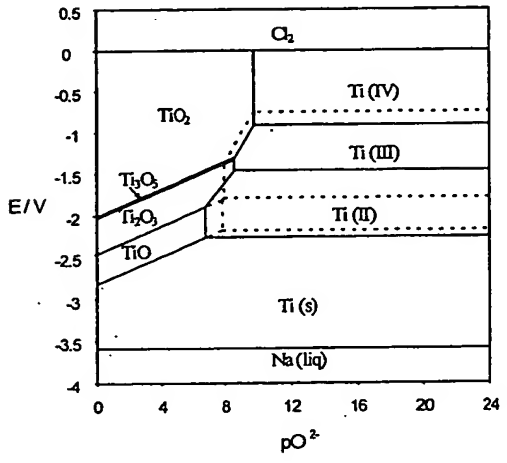

Fig. 13. Potential-pO^{2-} diagram for titanium in equimolar $CaCl_2$ + NaCl mixture at 550°C. Conditions: (——): $[Ti^{+3}]=1$ mol kg^{-1}; $[Ti^{+2}]=10^{-3}$ mol kg^{-1}; $P_{Ti(IV)}=1$ atm. (– – –): $[Ti^{+3}]=10^{-1}$ mol kg^{-1}; $[Ti^{+2}]=10^{-2}$ mol kg^{-1}; $P_{Ti(IV)}=1$ atm.

3.1.4. The diffusion coefficient of Ti(II)

The diffusion coefficients, $D_{Ti(II)}$, given in Table 7, were calculated from different electrochemical techniques by applying the appropriate equations. It has to be indicated that although a tungsten or molybdenum wire was used as working electrode, all the formulas used are relevant to planar semi-infinite diffusion because under the experimental conditions, the corrections related to cylindrical geometry can be neglected [41–44].

It is quite common for a process that is reversible at low sweep rates to become irreversible at higher ones after having passed through a region known as quasi-reversible at intermediate values [45]. This transition from reversibility occurs when the relative rate of the electron transfer with respect to that of mass transport is insufficient to maintain Nernstian equilibrium at the electrode surface. This change on the reversibility of the system can readily be seen from the plot of I_{pc} as a function of $v^{1/2}$. In this way, I_{pc} versus $v^{1/2}$ plots corresponding to the voltammograms obtained at tungsten and molybdenum substrates (see Fig. 11a) showed a change in the slope at the same value of the sweep rate for which we studied the reversibility of the system ($v>0.5$ and 0.7 V s^{-1} at molybdenum and tungsten electrodes, respectively).

We have demonstrated above that the electrodeposition of titanium is a quasi-reversible process. In that case, most authors consider that the Berzins-Delahay equation [46]:

$$I_p=0.61(nF)^{3/2}(RT)^{-1/2}Sc_oD^{1/2}v^{1/2} \quad (17)$$

for a reversible diffusion-controlled process can be used. When calculating the value of the diffusion coefficient from the slope of the plot I_p versus $v^{1/2}$, we obtained a value lower than those extracted from other electrochemical techniques (see Table 7) which indicates that in our conditions it is not fully correct to apply this equation.

As we said before, the convoluted curves obtained at different sweep rates exhibit a well defined limiting current, indicating that there is no significant change in the electrode surface area during the scan, i.e. the titanium deposit does not increase the surface of the electrode to the point that it affects the limiting current for the Ti(II) reduction wave. The Ti(II) diffusion coefficient was computed from the boundary semi-integral values by means of Eq. (11).

Chronopotentiometric studies of the reduction of Ti(II) ions obeyed Sand's law:

$$I\tau^{1/2}=\frac{1}{2}nFSc_oD^{1/2}\pi^{1/2} \quad (18)$$

Transition times for several current densities were measured [34] and the resultant I versus $1/\tau^{1/2}$ plot yielded a straight line, indicating that the fluxes of Ti(II) species

Table 9
Equilibrium potentials and values of standard potentials of redox systems of titanium in $CaCl_2$+NaCl equimolar melt at 550°C

System	Expression of the equilibrium potential	Standard potential vs Cl_2/Cl^- at 1 atm/V
$Ti(II)+2e^- \Leftrightarrow Ti(s)$	$E = E_1^\circ + \frac{2.3RT}{2F}\log[Ti(II)]$	$E_1^\circ = -2.013$
$Ti(III)+e^- \Leftrightarrow Ti(II)$	$E = E_2^\circ + \frac{2.3RT}{F}\log\left[\frac{Ti(III)}{Ti(II)}\right]$	$E_2^\circ = -1.945$
$Ti(IV)+e^- \Leftrightarrow Ti(III)$	$E = E_3^\circ + \frac{2.3RT}{F}\log\frac{P_{TiCl4}}{[Ti(III)]}$	$E_3^\circ = -0.909$
$TiO_2+e^- \Leftrightarrow Ti(III)+2O^{2-}$	$E = E_4^\circ - \frac{2.3RT}{2F}\log[Ti(III)] + \frac{2.3RT}{F}2pO^{2-}$	$E_4^\circ = E_3^\circ - \frac{2.3RT}{F}pK_s(TiO_2)\ldots E_4^\circ = -4.111$
$3TiO_2+2e^- \Leftrightarrow Ti_3O_5+O^{2-}$	$E = E_5^\circ + \frac{2.3RT}{2F}pO^{2-}$	$E_5^\circ = -1.995$
$Ti_3O_5+e^- \Leftrightarrow 3Ti(III)+5O^{2-}$	$E = E_6^\circ - \frac{2.3RT}{F}3\log[Ti(III)] + \frac{2.3RT}{F}5pO^{2-}$	$E_6^\circ = E_3^\circ - \frac{2.3RT}{F}pK_s(Ti_3O_5)\ldots E_6^\circ = -8.413$
$2Ti_3O_5+2e^- \Leftrightarrow 2Ti_2O_3+O^{2-}$	$E = E_7^\circ + \frac{2.3RT}{2F}pO^{2-}$	$E_7^\circ = -2.032$
$Ti_2O_3+2e^- \Leftrightarrow 2Ti(II)+3O^{2-}$	$E = E_8^\circ - \frac{2.3RT}{2F}2\log[Ti(II)] + \frac{2.3RT}{2F}3pO^{2-}$	$E_8^\circ = E_2^\circ - \frac{2.3RT}{F}pK_s(Ti_3O_5)\ldots E_8^\circ = -9.449$
$Ti_2O_3+2e^- \Leftrightarrow 2TiO+O^{2-}$	$E = E_9^\circ + \frac{2.3RT}{2F}pO^{2-}$	$E_9^\circ = -2.450$
$TiO+2e^- \Leftrightarrow Ti(s)+O^{2-}$	$E = E_{10}^\circ + \frac{2.3RT}{2F}pO^{2-}$	$E_{10}^\circ = E_1^\circ - \frac{2.3RT}{F}pK_s(TiO)\ldots E_{10}^\circ = -2.814$

were diffusion controlled (see Fig. 11b), and from which slope we could determine the diffusion coefficient.

3.2. Stability of pure titanium oxides and equilibrium potential-pO^{2-} diagram of titanium

A knowledge of the oxo-acidity properties in the molten salt mixtures also allows their influence on the oxidation-reduction and electrochemical properties to be predicted. As emphasized before [47–55] the main phenomena can be expressed in diagrams of equilibrium potential versus pO^{2-}.

The composition of titanium oxides as well as their solubility products can be theoretically determined by analysis of the curves for potentiometric titration of oxide ion with an oxoacid (Lux-Flood oxoacidity [56,57]) or viceversa. The variation of pO^{2-} (equal to the cologarithm of oxide ion activity) was measured experimentally by means of an yttria-stabilized zirconia membrane electrode (YSZME) which has a Nernstian behaviour in this melt [28].

In order to determine the solubility product of TiO, K_{s1}, we have carried out the titration of Ti^{2+} by O^{2-} ions (added as sodium carbonate) (Fig. 12a). The potential values of the YSZME show only one equivalence point α (defined as the ratio of added ion and the initial Ti(II) concentration, c_o) equal to 1. The corresponding solubility products were determined by applying the Gauss-Newton non-linear least-squares method to the equation of the corresponding titration curve. The value obtained is shown in Table 8.

The experimental titration curve for solid $TiCl_3$ against O^{2-} was obtained in the same way. The potential values obtained after successive additions of known amounts of sodium carbonate to a solution of Ti(III) with an initial concentration $c_o = 0.02476$ mol kg^{-1} are plotted in Fig. 12b. Only one equivalence point can be observed for a stoichiometric ratio

$$\alpha[CO_3^{2-}]_{added}/[TiCl_3]_{initial} = 1.5 \quad (19)$$

Table 10
Equilibrium potentials and values of standard potentials of some redox systems in the equimolar $CaCl_2+NaCl$ melt (potentials versus Cl_2/Cl^- at 1 atm; molality scale; pressure, atm; T, K)

System	Expression for equilibrium potential	Standard potential, $E°/V$ ($T=550°C$)
$2Cl^- - 2e^- \leftrightarrow Cl_2$ (g)	$E = E_o^\circ + 2.3RT\cdot(2F)^{-1}\log P(Cl_2)$	$E_o^\circ = 0$
$O^{2-} - 2e^- \leftrightarrow 1/2O_2$ (g)	$E = E_1^\circ + 2.3RT\cdot(4F)^{-1}\log P(O_2) + 2.3RT\cdot(2F)^{-1}pO^{2-}$	$E_1^\circ = -0.466$
H_2 (g) $- 2e^- + 2Cl^- \leftrightarrow 2HCl$	$E = E_2^\circ + 2.3RT\cdot F^{-1}\log P(HCl) - 2.3RT\cdot(2F)^{-1}\log P(H_2)$	$E_2^\circ = -1.033$
C (s) $- 2e^- + O^{2-} \leftrightarrow CO$ (g)	$E = E_3^\circ + 2.3RT\cdot(2F)^{-1}\log P(CO) + 2.3RT\cdot(2F)^{-1}pO^{2-}$	$E_3^\circ = -1.422$
C (s) $- 4e^- + 2O^{2-} \leftrightarrow CO_2$ (g)	$E = E_4^\circ + 2.3RT\cdot(4F)^{-1}\log P(CO_2) + 2.3RT\cdot(2F)^{-1}pO^{2-}$	$E_4^\circ = -1.491$
CO (g) $- 2e^- + 2O^{2-} \leftrightarrow CO_2$ (g)	$E = E_5^\circ + 2.3RT\cdot(2F)^{-1}\log(P(CO_2/P(CO)) + 2.3RT\cdot(2F)^{-1}pO^{2-}$	$E_5^\circ = -1.559$
H_2 (g) $- 2e^- + 2O^{2-} \leftrightarrow H_2O$ (g)	$E = E_6^\circ + 2.3RT\cdot(2F)^{-1}\log(P(H_2O)/P(H_2)) + 2.3RT\cdot(2F)^{-1}pO^{2-}$	$E_6^\circ = -1.514$

Table 11
Main chlorination equilibria and values of their equilibrium constants (molality scale; partial pressure, atm; T, K)

Gaseous mixture	Equilibrium	Log $K°$
Cl_2 (g) + O_2 (g)	Cl_2 (g) + $O^{2-} \leftrightarrow 1/2O_2$ (g) + $2Cl^-$	$(-2F/2.3RT)\ E°(1/2O_2/O^{2-}) = 5.71$
Cl_2 (g) + C (s)	Cl_2 (g) + $1/2C$ (s) + $O^{2-} \leftrightarrow 1/2CO_2$ (g) + $2Cl^-$	$(-2F/2.3RT)\ E°(CO_2/C) = 18.27$
Cl_2 (g) + CO (g)	Cl_2 (g) + CO (g) + $O^{2-} \leftrightarrow CO_2$ (g) + $2Cl^-$	$(-2F/2.3RT)\ E°(CO_2/CO) = 19.11$
HCl (g) + H_2O (g)	2HCl (g) + $O^{2-} \leftrightarrow H_2O$ (g) + $2Cl^-$	2 log P(HCl) − log P(H_2O) − pO^{2-} = 5.9 (P(HCl) = 1 atm; P(H_2O) = 10^{-2} atm)
HCl (g) + CO (g) + H_2 (g)	2HCl (g) + CO (g) + $O^{2-} \leftrightarrow CO_2$ (g) + H_2 (g) + $2Cl^-$	$(2F/2.3RT)\ [E°(2HCl/H_2) - Eo(CO_2/CO)] = 6.45$
HCl (g) + H_2 (g) + H_2O (g)	2HCl (g) + $1/2H_2$ (g) + $O^{2-} \leftrightarrow H_2O$ (g) + $2Cl^-$	$(2F/2.3RT)\ [E°(2HCl/H_2) - E°(H_2O/H_2)] = 5.89$

This value indicates that the reaction is:

$$2Ti^{3+} + 3O^{2-} \leftrightarrow Ti_2O_3\ (s) \qquad (20)$$

and it can be deduced that no oxychloride species were stable under the conditions used. This is in agreement with the thermodynamic data.

From the mass balance equations:

$$[O^{2-}]_{bulk} = [O^{2-}]_{add} - 3[Ti_2O_3]_{ppt} \qquad (21)$$

$$[Ti(III)]_{bulk} = [Ti(III)]_{initial} - 2[Ti_2O_3]_{ppt} \qquad (22)$$

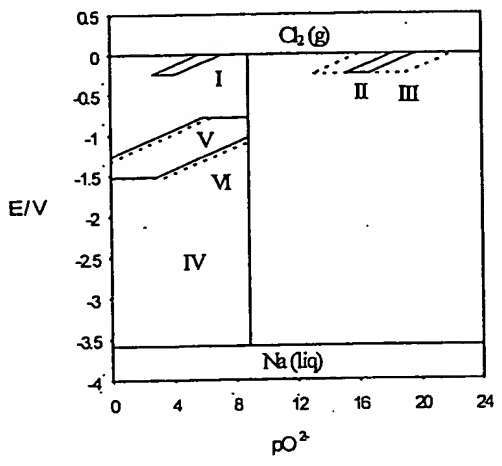

Fig. 14. Potential-pO^{2-} diagram for some gaseous mixtures in $CaCl_2+NaCl$ equimolar mixture at 550°C at partial pressures in range $1-10^{-3}$ atm. Mixtures: I: Cl_2+O_2; II: Cl_2+CO; III: $Cl_2+C(s)$; IV: $HCl+H_2O$; V: $HCl+H_2O+H_2$; VI: $HCl+H_2+CO$.

and with the expression of the solubility product, $K_{s\,2} = [Ti(III)]^2_{bulk}[O^{2-}]^3_{bulk}$, we can derive an equation for the titration curve:

$$[O^{2-}]^5 - 2c_o(\alpha - 3/2)[O^{2-}]^4 + c_o^2(\alpha - 3/2)^2[O^{2-}]^3 - 9/4K_{s\,2} = 0 \qquad (23)$$

The $K_{s\,2}$ value was calculated by applying the corresponding equation of the titration curve to the experimental points obtained during the titration of solid $TiCl_3$ by O^{2-} before the equivalence point. Under these conditions, Eq. (23) can be written as follows:

$$pO^{2-} = \frac{1}{3}\log\left[K_{s\,2}/c_o^2\left(1-\frac{2}{3}\alpha\right)^2\right] \qquad (24)$$

c_o being the initial $TiCl_3$ concentration.

The mean value of $pK_{s\,2}$ obtained from different titrations is shown in Table 8.

It was not possible to study experimentally the stability of TiO_2 due to the instability of Ti(IV) solutions in our melt. However we have determined it by means of the stability constant K_3^* for the reaction between pure compounds:

$$TiO_2\ (s) + 2Na_2O\ (s) \leftrightarrow TiO_2\ (s) + 4NaCl\ (s) \qquad (25)$$

by using the relation:

$$pK_{s\,3} = pK^*_{s\,3} + 2\log f(Na_2O) - 4\log a(NaCl) \qquad (26)$$

where $pK^*_{s\,3}$ was calculated from the chemical potentials given in the literature [58]. The activity coefficient of Na_2O was derived from obtained experimental data. The value so obtained is given in Table 8.

The data given in Table 8 as well as the standard potential values of the electrochemical couples Ti(III)/Ti(II) and Ti(II)/Ti(0) (obtained previously in Sections 3.1.2 and 3.1.3, respectively) were used to build up the equilibrium potential-acidity diagrams for Ti-O compounds (Fig. 13 and Table 9). It clearly shows the great stability of (II) and (III) oxidation states of titanium as well as the strong acidity of titanium chlorides.

3.3. Chlorinating and oxidizing powers of gaseous mixtures

As it was done in earlier studies in the LiCl + KCl eutectic [59–63], we have characterized several gaseous mixtures that can be used as chlorinating agents according to their oxoacidic and redox properties (Tables 10 and 11). Among them, we can distinguish two groups of reagents on the basis of the range of pO^{2-} conditions that they produce (see Fig. 14):

- Group I. It gives pO^{2-} values in the range 5.7–12.5 and includes chlorine-based mixtures (Mixture I) which are strongly oxidizing and hydrogen-based mixtures (Mixtures V and VI) which are reducing (potential value close to -1.5 V).
- Group II. It comprises $CO(g) + Cl_2(g)$ mixtures and phosgene. These are the most reactive (i.e. the most strongly chlorinating and oxidizing agents). A similar effect is obtained with chlorine in the presence of solid carbon.

4. Conclusions

Our study confirms the stability of the oxidation states of titanium: 0, II and III in the equimolar mixture $CaCl_2 + NaCl$ at 550°C. Ti(IV) was found to be unstable in the melt, probably due to the low solubility of gaseous $TiCl_4$.

Using electrochemical techniques it was possible to determine accurately the kinetic parameters characterizing the mass and the charge transfers occurring in the electrochemical reduction of Ti(III) and Ti(II) ions at different substrates.

The results showed that mass transport towards the electrode is a simple diffusion process and that the diffusion coefficients of both electroactive species (Ti(III) and Ti(II)) are close to each other, which is in agreement with the results obtained by other authors in other molten chlorides. However, discrepancies were found in the kinetics of the processes. We have calculated the values of the charge-transfer kinetic parameters from the logarithmic analysis of convoluted curves by applying the equations corresponding to a quasi-reversible process in both Ti(III)/Ti(II) and Ti(II)/Ti(0) exchanges and also by using a simulation computer program in the case of the soluble-soluble system. The values of the k^o and α so obtained showed that although both electrochemical systems are quasi-reversible at all the substrates studied, the Ti(III)/Ti(II) exchange is closer to the reversibility than the titanium electrodeposition process. That can also explain why Eq. (17) leads to lower values of the Ti(II) diffusion coefficients than those calculated by other electrochemical techniques such as convolution or chronopotentiometry.

Chronoamperometric studies indicated instantaneous nucleation and crystal growth of titanium at tungsten electrodes.

Since in the reversibility studies of the Ti(II)/Ti(0) system we use criteria corresponding to the electrodeposition of an insoluble product which do not take into account the nucleation of the product phase, we can think that the quasi-reversibility of that exchange can be due to the nucleation phenomena overpotential, or that this gives some irreversibility to the electrodeposition process. However, we should emphasize that we have applied the reversibility criteria to those cases where under the given experimental conditions the nucleation phenomena do not occur. Therefore the values of the kinetic parameters are exclusively due to the quasi-reversibility of the process.

The standard potentials of the redox couples Ti(III)/Ti(II) and Ti(II)/Ti(0) have been determined by voltammetry where the systems showed a reversible behaviour. The values so obtained were: E_1° (Ti(II)/Ti(0)) = -2.013 ± 0.030 V and E_2° (Ti(III)/Ti(II)) = -1.945 ± 0.030 V versus the Cl_2/Cl^- electrode system, and allowed us to calculate the equilibrium constant, K, of the disproportionation of Ti(II):

$$3Ti(II) \leftrightarrow 2Ti(III) + Ti\,(s) \quad (27)$$

according to the equation:

$$\log K = 2F(E_1^\circ - E_2^\circ)/2.3RT \quad (28)$$

The value so obtained was $K = 10^{-0.83}$.

On the other hand from the data given in Table 9, we could also verify that the other disproportionation reactions proposed by Chassaing et al. [14] do not take place under our experimental conditions.

Moreover, the stability of titanium oxides was investigated. The solubility products of both TiO and Ti_2O_3 were determined experimentally by potentiometric titration of titanium (II) and (III) ions, respectively, by sodium carbonate. The pK_s of titanium dioxide was determined combining experimental and thermodynamic data.

The equilibrium potentials and values of standard potentials of redox systems of titanium as well as solubility products of titanium oxides were used to build-up the potential-pO^{2-} diagram which summarizes the properties of Ti-O compounds in the melt studied, the equimolar $CaCl_2 + NaCl$ mixture at 550°C.

From a comparison of this diagram and that from some gaseous mixtures it is possible to predict operating conditions for the process of industrial production of metallic titanium from salt systems (chlorination of rutile and subsequent electrowinning of metallic titanium). It is evident that to chlorinate the very stable oxide TiO_2 requires one of the most reactive mixtures, Cl_2 (g) + CO (g) (phosgene) or Cl_2 (g) + C (s). The product obtained is $TiCl_4$, regardless of the partial pressures of the different gaseous components.

Acknowledgements

The authors are grateful to DGICYT UE93-0017, DGES PB96-0364 and Junta de Castilla y León (Spain) for financial support which enabled this study. A.M. Martínez wishes also to thank DGICYT for a doctoral grant.

References

[1] W.J. Kroll, The production of ductile titanium, Trans. Electrochem. Soc. 78 (1940) 35–46.
[2] J.A. Menzies, D.L. Hill, G.J. Hill, J. Young, J. Bockris, J. Electroanal. Chem. 1 (1959) 161.
[3] W.E. Reid, J. Electrochem. Soc. 108 (1957) 393.
[4] F. Ouemper, D. Deroo, N. Rigard, J. Electrochem. Soc. 119 (1972) 1353.
[5] E. Chassaing, F. Basile, G. Lorthiair, J. Less-Com. Metals 68 (1979) 153.
[6] S. Tokumoto, E. Tanaka, O. Ogisu, J. Metall. 27 (1974) 175.
[7] S. Mori, T. Kuroda, K. Kawamura, Denki Kagaku 42 (1974) 175.
[8] M.B. Airpert, F.J. Shultz, W.F. Sullivan, J. Electrochem. Soc. 104 (1957) 555.
[9] M.B. Airpert, J.A. Hamilton, F.J. Shultz, W.F. Sullivan, J. Electrochem. Soc. 106 (2) (1959) 142.
[10] K. Komarek, P. Herasynenko, J. Electrochem. Soc. 105 (4) (1958) 210.
[11] M.V. Smirnov, O.V. Skiba, Electrochemistry of molten and solid electrolytes, vol. 2, Consultants Bureau, New York, 1964, p.21.
[12] S.N. Flengas, Ann. NY Acad. Sci. 79 (1960) 853.
[13] M.J. Rand, L.J. Reimert, J. Electrochem. Soc. 111 (1964) 429.
[14] E. Chassaing, F. Basile, G. Lorthoir, J. Appl, Electrochem. 11 (1981) 187.
[15] C.A.C. Sequeira, J. Electroanal. Chem. 239 (1988) 203.
[16] H. Wendt, K. Reuhl, V. Schwartz, Electrochim. Acta 37 (1992) 237.
[17] W.K. Rolland, Electrodeposition of titanium from alkali chloride containing di- and tri-valent titanium chloride, Thesis, Department of Electrochemistry, NTH, Trondheim, Norway, 1987.
[18] G.M. Haarberg, W. Rolland, A. Sterten, J. Thonstad, J. Appl. Electrochem. 23 (1993) 217.
[19] D.M. Ferry, Thèse de Doctorat de l'Université Paris 6, 1985.
[20] D.M. Ferry, G.S. Picard, B. Trémillon, Trans. Inst. Min. Metall. C Min. Proc. Ext. Metall. 97 (1988) C21.
[21] S. Vire, Electrochemical studies of titanium in molten chlorides and fluorides. PhD thesis, Dept. Metallurgy and Material Science, Imperial College, June 1981, p. 293.
[22] F.R. Claiton, G. Mamantov, D.L. Manning, J. Electrochem. Soc. 120 (1973) 1199.
[23] D. Schlain, F.X. McCawley, C. Wyche, J. Electrochem. Soc. 116 (1969) 1227.
[24] S. Okada, M. Kawane, T. Hashino, Z. Elektrochemie 62 (1958) 437.
[25] K.W. Fung, G. Mamantov, J. Electroanal. Chem. 35 (1972) 27.
[26] Y. Castrillejo, A.M. Martínez, G.M. Haarberg, B. Børresen, K.S. Osen, R. Tunold, Electrochim. Acta 42 (10) (1997) 1489.
[27] Y. Castrillejo, A.M. Martínez, R. Pardo, G.M. Haarberg, Electrochim. Acta 42 (12) (1997) 1869.
[28] J.Lumsden, Thermodynamics of Molten Salts Mixtures, Academic Press, New York, 1966.
[29] J.C. Gabriel, J. Bouteillon, J.C. Poignet, J.M. Roman, J. Electrochem. Soc 141 (9) (1994) 2286.
[30] J. Osteryoung, R.A. Osteryoung, Anal. Chem. 57 (1985) 101.
[31] L. Ramaley, M.S. Krasue, Anal. Chem. 41 (1969) 1362.
[32] G.C. Barker, Anal. Chim. Acta 18 (1958) 118.
[33] J. Osteryoung, J.J. ODea, Electroanal. Chem. 14 (1986) 209.
[34] A.J. Bard, L.R. Faulkner, Electrochemical Methods, Wiley, New York, 1980.
[35] J.C. Imbeaux, J.M. Savéant, J. Electroanal. Chem. 44 (1973) 169.
[36] D.D. McDonald, Transient Techniques in Electrochemistry, Plenum Press, New York, 1977.
[37] H. Matsuda, Y. Ayabe, Z. Electrochem. 59 (1955) 494.
[38] J. O'Dea, J. Osteryoung, T. Lane, J. Phys. Chem. 90 (1986) 2761.
[39] Y. Castrillejo, A.M. Martínez, M. Vega, E. Barrado, G. Picard, J. Electroanal. Chem. 397 (1995) 139.
[40] G. Gunawardena, G. Hills, I. Montenegro, B. Scharifker, J. Electrochem. Soc. 138 (1982) 225.
[41] Z. Galus, Fundamental of Electrochemical Analysis, Wiley, New York, 1976.
[42] D.G. Peters, J.J. Lingane, J. Electroanal. Chem. 2 (1961) 1.
[43] K.B. Oldham, J. Electroanal. Chem. 41 (1973) 351.
[44] D.H. Evans, J.E. Price, J. Electroanal. Chem. 5 (1963) 77.
[45] Instrumental Methods in Analytical Chemistry, Southampton Electrochemistry Group, Ellis Horwood, London, 1990.
[46] G. Mamantov, D.L. Manning, J.M. Dale, J. Electroanal. Chem. 9 (1965) 253.
[47] R. Littlewood, J. Electrochem. Soc. 109 (1962) 525.
[48] M. Ingram, G. Janz, Electrochim. Acta 10 (1965) 783.
[49] J. Goret, B. Tremillon, Electrochim. Acta 12 (1967) 1065.
[50] A. Conte, M. Ingram, Electrochim. Acta 13 (1968) 1551.
[51] A. Rahmel, Electrochim. Acta 13 (1968) 495.
[52] G. Bombara, G. Baudo, A. Tamba, Corros. Sci. 8 (1968) 393.
[53] A. Eluard, B. Tremillon, J. Electroanal. Chem. 18 (1968) 277.
[54] A. Eluard, B. Tremillon, J. Electroanal. Chem. 26/27 (1970) 117–259.
[55] B. Tremillon, Pure Appl. Chem. 25 (1971) 395.
[56] H.Z. Lux, Elektrochemie 45 (1939) 303.
[57] H. Flood, T. Förland, The acidic and basic properties of oxides, Acta Chem. Scand. 1 (1947) 592.
[58] J. Barin, O. Knacke. Thermochemical Properties of Inorganic Substances, Springer, Berlin, 1973.
[59] F. Seon, G. Picard, B. Tremillon, Electrochim. Acta 28 (1983) 209.
[60] F. Seon, Thèse de Doctorat de l'Université Paris 6, 1981.
[61] F. Seon et al., French patent 2 514 028, 1983.
[62] G. Picard, F. Seon, B. Tremillon, Proc. Electrochem. Soc. Molten Salts 84 (2) (1984) 694.
[63] B. Tremillon, G. Picard, English abstract, Rare Metals 4 (2) (1985) 29.